Chapter 3 2D flood modelling with Delft-FLS

The previous chapter presented the conceptual framework for hazard and risk assessment. This chapter will deal with an important tool for simulating flood events in complex terrain: a 2D flood propagation model. Such a model offers possibilities to quantify the dynamics of a flood event and to run different scenarios to evaluate the consequences of certain actions (or in-actions). These analysis may then be used as basis for decision-making and flood-risk assessment.

Abstract

This chapter presents the theoretical and practical basis for the application of 2D hydraulic models for flood hazard assessment. It first deals with the specific needs of flood hazard assessment, and what this implies for the choice of modelling approach. The second section describes the selected model – Delft-FLS - in more detail. Finally the general data management environment is described in which the modelling is embedded. The model needs spatial and temporal input data and it generates a large amount of spatial-temporal output data in the form of map-series with the spatial and temporal changes in water depth and flow velocity. For the management of these input and output data a GIS is required for storage, processing and analysis.

3.1 The need for 2D-models

In section 2.2 a geomorphologic hazard was defined as the probability that a certain geomorphologic process will occur in a certain area with a certain intensity within a given period of time. To translate this to floods, one can define flood hazard as the probability that a certain area will be inundated within a given period of time. Thus, traditional flood hazard maps delineate the annual chance of inundation, as shown in the top part of Figure 3.1. In this situation there is an inverse relationship between water level and chance of occurrence: the higher the water level the smaller the chance that it happens. In Figure 3.1 location A is more hazardous than location D.

In the lower part of Figure 3.1 the "Polder" situation is depicted, a situation that can be found in all major river delta areas, coastal plains and alluvial plains in the world where the river is flanked by widespread near-flat terrain. In some cases the surrounding terrain lies below the level of the river as a result of different subsidence characteristics between the more sandy deposits in and along the riverbed and the clayey, peaty deposits in the back-swamp areas. Often this difference in height is enhanced by artificial drainage of the back-swamps that leads to further subsidence.

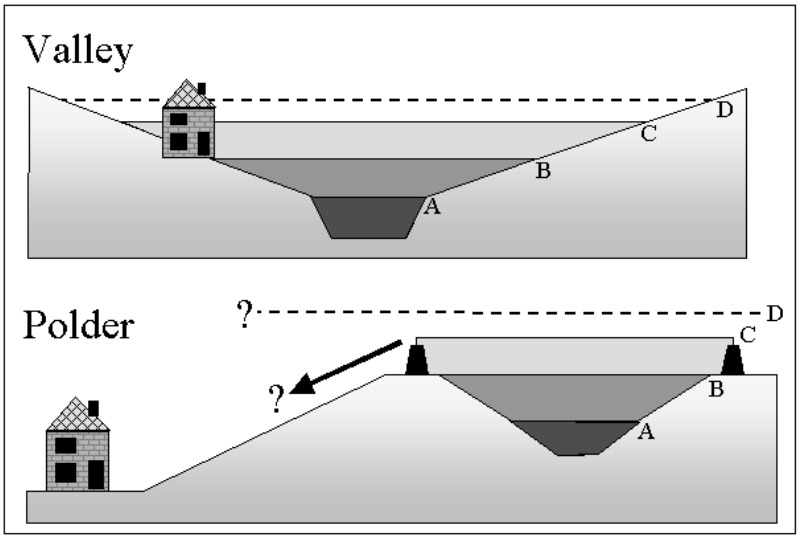

Figure 3.1 Morphological differences between upstream and downstream surface topography and its consequences for flood hazard zonation.

In the "polder" situation there is only a relation between the water level and return period of the flood as long as the river water does not overtop or breach the natural levees (B) or the dikes (C). A traditional hazard map equals the hazard in the whole polder area as the chance that the dikes are. This approach does not allow the differentiation in degrees of hazard within the alluvial plain (or polder) because it does not consider the propagation of the inundation flow. Clearly, the water level D in the lower part of Figure 3.1 is not instantly achieved in the whole flooded alluvial plain or polder. It takes time to fill the bathtub. How much time depends on the flux of water into the area and the characteristics of the terrain, like resistance to overland flow and the presence of obstacles like buildings,

embankments, etc. This temporal component is essential for decision-makers because people living in areas that are inundated within hours are more "at risk" than people living further on that have still days to respond to the hazard. Authorities need to know in advance which people to evacuate first and which roads are still accessible. Traditional flood hazard maps do not provide the right information to develop such evacuation plans. Furthermore they offer no help to planners to analyse the impact of new developments within these areas on possible future inundations. Simulating scenario floods with a 2D flood propagation model can help in these cases.

3.2 Numerical flood simulation

To quantify the flow of water as function of the topography, physically based hydrodynamic or hydraulic models are needed. Such models are based on the principle of conservation of mass, momentum and energy. Even though the theory was developed in the 17th to 19th century by Isaac Newton (1643-1727), Claude-Louis Navier (1785-1836), Adhémar Jean Claude Barré De Saint Venant (1797-1886) and George Gabriel Stokes (1819-1903), the modelling of the flow of water over initially dry areas is still extremely complicated (Alcrudo and Garcia Navarro, 1994), not in the least because no analytical solutions have been found yet for the full 3D unsteady Navier-Stokes non-linear partial differential equations. This set of equations relate the motion of fluids and gasses to viscosity, pressure, gravity and other internal and external forces. The equations are rather generic as they apply to all kinds of fluid-like substances that can range from the flow of air to the motion of stars in a galaxy. For applications in flood studies certain assumptions can be made to derive a new set of equations that are specifically applicable to the flow of inviscid water, like shallow depth of the flow compared to its width and that the bottom slope is relatively small. In these cases flood modelling can be done using the 3D shallow water flow equations of De Saint Venant (1871).
Furthermore, for flood applications it is often not needed to have information on the vertical velocity profile and on water flow in the vertical direction. This simplification allows the omission of the vertical (z-) component from the equations. For channel flow modelling one may then further reduce the number of dimensions by assuming that there is no flow perpendicular to the main direction of the river, so that flow is calculated in only one direction.

One-dimensional flow

When considering channel flow, it is assumed that the flow behaviour can be satisfactorily described as unsteady flow (flow characteristics may change over time) in one spatial dimension by 2 state variables: velocity (u) and water depth (h) as function of time (t) and space (x), while taking into account the following additional assumptions (Stelling and Verwey, 2005):

- Discharge is the integral of the velocities through a cross-section, perpendicular to the axis of flow (x-direction);
- The water level is constant along the cross-section: all water movement up and down happens at the same rate. There is no flow calculated perpendicular to the axis of flow;
- The pressure distribution in the vertical is hydrostatic;
- Water density is considered constant;
- The resistance relationship for steady flow is also applicable for unsteady flow;
- The bed slope is not too step (cosine of the slope is approximately 1).

The Saint-Venant equations

To solve u and h, two independent equations are required and usually the continuity equation (based on the conservation of mass principle) and the momentum equation (based on the conservation of momentum principle) are used. These two equations derived by De Saint Venant in 1871 are shown below in their Eulerian form per unit width of channel with no lateral inflow:

$$\frac{\partial(h+z_b)}{\partial t}+\frac{\partial(uh)}{\partial x}=0 \qquad 3.1$$

$$\frac{\partial u}{\partial t}+u\frac{\partial u}{\partial x}+g\frac{\partial(h+z_b)}{\partial x}+c_f\frac{u|u|}{h}=0 \qquad 3.2$$

Where:

x is the position along the channel axis (m); **t** is time (s), **u** is the velocity vector in the x-direction (m/s), **h** is the water depth (m), $\mathbf{z_b}$ is the local bottom level above the reference datum, $\mathbf{c_f}$ is the dimensionless bottom friction coefficient and **g** is the constant of gravity (9.81 m^2/s).

Stelling and Verwey (2005) give the following meaning to the terms in the equations: the first term in formula 3.1 represents the rate of volume stored over a unit length of channel. The second term accounts for the rate at which the discharge changes along the channel per unit of time. In formula 3.2 the first term represents the change of momentum in a control volume of unit length of channel and reflects the inertia of the water mass present in that control volume. The second term is called the convective momentum term and reflects the balance of momentum flowing through the control volumes' upstream and downstream cross-section. The third term combines the effect of impulses generated by differences in upstream and downstream hydrostatic forces (hydrostatic pressure term) and the gravity acting on the mass in the control volume (gravity term) and the last term is the so-called friction term that represents the effect of channel friction. Solutions based on the full set of equations (3.1 and 3.2) are defined as the full dynamic wave description (Stelling and Verwey, 2005).

Numerical solutions of the full dynamic wave description

Modern 1D hydraulic models are based upon numerical solutions of the full dynamic wave description. This is largely a result of the rise of fast and cheap computation power in the 1990s. The search for robust numerical solutions follows many paths as can be demonstrated by the enormous amount of publications in this field (e.g. Alcrudo and Garcia Navarro, 1994; Hervouet and Janin, 1994; Benkhaldoun and Monthe, 1994; Di Giammarco and Todini 1994; Bates and De Roo, 2000; Horritt and Bates, 2002; Dresback et al. 2005, Stelling and Verwey (2005), Kamrath et al. 2006). Along the path the modellers make choices regarding:

a) The discretization form of the problem;
b) The computation of the derivatives, using implicit or explicit difference methods;
c) The use of staggered or non-staggered schemes solutions;
d) Approximation of the convective momentum term in equation 3.2;
e) Estimation of the computational time step (dt).

Ad a). The most widely used forms of discretization are finite difference methods, finite element methods and the finite volume methods. Finite difference methods can be used in a grid environment whereas finite element and finite volume methods require a mesh representation. All have in common that infinitesimal small increments in space and time are replaced by discrete finite increments that

give an approximate of the differential equation (finite difference method) or its solution (finite elements and finite volume methods). The applicability of either method depends on the problem. Finite difference methods are simpler to apply and work well in cases the problem can be represented well by a simple geometry (like a grid). Finite elements methods can handle more complex geometries.

Ad b). There are several ways to compute the derivatives in the equations. Explicit methods use a so-called forward difference in time and compute the state of the system as a function of the previous state. Implicit methods use a so-called backward difference at each computational time step to find the solution involving both the current state and the future state. Although the explicit solution is easier to implement, the implicit method is more frequently applied because it offers robust solutions with larger time steps than the explicit methods. The extra computations that the implicit method needs balance the smaller time-steps required by the explicit method to achieve the same accuracy. Stelling and Verwey (2005) state that implicit methods offer advantages regarding unconditional numerical stability and that it solves satisfactorily the robustness problems related to non-linear effects and flooding and drying of channels and floodplains.

Ad c). Staggered and non-staggered grids relate to the spatial and temporal representation of the two state variables v and h. When these two are computed at the same grid points (cells), the grid is so-called non-staggered. In contrast the grid is called staggered when the state variables are computed on alternating grid points. It has been shown by e.g. Stelling et al. (1998) that the staggered grid offers advantages by guaranteeing the convergence of the numerical solutions and the better ability to handle flooding and drying of grid cells (see also Stelling and Verwey, 2005).

Ad d). The non-linear convective momentum term in equation 3.2 requires a transformation. Stelling and Duinmeijer (2003) state that the correct formulation depends on the way in which the convective speed of momentum is interpolated on the grid. This results in an approximation that is only first order accurate whereas the numerical discretization is other terms in the Saint Venant equations are second order accurate. For most practical applications this lower accuracy is quite acceptable, although locally the convective momentum term can become dominant. Most advanced models have specific solutions for these local conditions.

Ad e). The incremental time-step dt has to be defined to compute the state of the system at the next time step. The incremental time-step can be *a priori* user-defined like the incremental spatial step dx. However more robust ways of estimating dt are based on the state of the system at a previous time-step. In these cases the time-step is estimated using the Courant number condition where dt <= dx/Vmax. According to Stelling and Verwey (2005) this approach has as the advantage that newly computed water levels can never fall below the bottom of the channel, thus avoiding negative water depths.

Two-dimensional flow

The basic assumptions discussed in the previous section also apply to the 2D shallow water equations. In their 2D Eulerian form, per unit width of the channel and neglecting lateral flow, the continuity equation (formula 3.3) and the momentum equations (3.4 and 3.5) read:

$$\frac{\partial h}{\partial t} + \frac{\partial (uh)}{\partial x} + \frac{\partial (vh)}{\partial y} = 0 \qquad 3.3$$

$$\frac{\partial u}{\partial t} + u\frac{\partial u}{\partial x} + v\frac{\partial u}{\partial y} + g\frac{\partial (h + z_b)}{\partial x} + c_f \frac{u\sqrt{u^2 + v^2}}{h} = 0 \qquad 3.4$$

$$\frac{\partial v}{\partial t} + u\frac{\partial v}{\partial x} + v\frac{\partial v}{\partial y} + g\frac{\partial (h + z_b)}{\partial y} + c_f \frac{v\sqrt{u^2 + v^2}}{h} = 0 \qquad 3.5$$

Where

x and **y** represent the orthogonal axis and **u** and **v** the velocity vectors along these axis respectively. The staggered grid shown in Figure 3.2, shows that water level (h) and flow velocity vectors (u and v) are computed at alternating grid points. The flow velocity (V) can easily be computed as the vector sum of the vector velocities u and v:

$$V = (u^2+v^2)^{1/2} \qquad 3.6$$

It should be noted that this schematisation of the problem computes water flow only towards the 4-connected cells and that no flow is calculated to the diagonals (8-connected cells). In the input data preparation this requires attention. Stelling and Duinmeijer (2003) and Stelling and Verwey (2005) give a thorough description of the way the numerical solutions of the 2D Saint Venant equations are implemented in Delft-FLS.

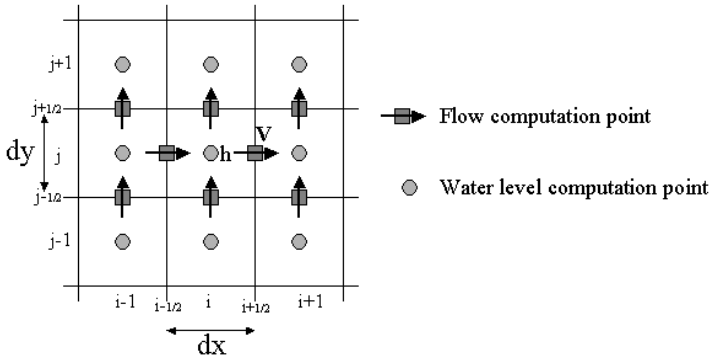

Figure 3.2. Staggered grid schematisation for 2D flow simulations

3.3 Delft-FLS

Delft-FLS - developed at WL|Delft Hydraulics - is a 2D hydrodynamic simulation package based on the full 2D shallow water equations that are solved using the finite difference method on a rectangular staggered grid. A description of the applied numerical solutions is given in Stelling et al. (1998) and Hesselink et al. (2003). In Stelling et al. (1998) is described how problems regarding water fronts or bores and hydraulics jumps are solved efficiently, which is especially relevant for inundations as a result of dam breaches. The scheme used in Delft-FLS is based upon the following characteristics (Hesselink et al. 2003):

- The continuity equation is approximated in such a way that (a) mass is conserved not only globally but also locally and (b) the total water depth is guaranteed to be always positive which excludes the necessity of "flooding and drying" procedures.
- The momentum equation is approximated in such a way that a proper momentum balance is fulfilled near large gradients.

The combination of positive water depths and mass conservation assures a stable numerical solution that converges thanks to the momentum balance. Given the approximations, Delft-FLS has a wide range of applications (Stelling et al. 1998), including practical problems such as overland flow, dam breaches, hydraulic jumps, flooding and drying of tidal flats, tidal bores etc. It adheres to the velocity Courant number as an automated time-step estimator, which reduces or enlarges the computational time step according to the flow characteristics at any moment during the simulation. Therefore it is efficient for most free surface flows, including flows in complex networks (Stelling et al. 1998). Because Delft-FLS computes on a rectangular grid, geometrical input data can be specified in a number of ways and land layout features such as dikes, roads, railroads, waterways, viaducts etc. can easily be included in the analysis. The user can force dike failures so that "what-if" scenarios can be investigated.

3.4 Input data

The implementation of 2D propagation models for flood hazard assessment is a complex process because of the handling of large amounts of spatial and non-spatial data. In this study a Geographical Information System (GIS) is used in parallel with the flood model to pre-process the data required as input for the model, as well as to post-process the model results and transform them into flood parameter maps – see Figure 3.3. This section describes the generation of the input data required for the model, using a flood study in Trento, Italy as example.

The Trento example

The city of Trento was severely flooded in 1966. Based on information and data provided by the Local and Regional Authorities in Trento, this event was reconstructed, using the 1966 surface topography and boundary conditions. In a second model run the 1966 event was simulated using the present (2000) topography where the city of Trento has expanded into the floodplain and major infrastructures have been constructed (Brenner highway and the Trento-Bypass road). Differences in the flood characteristics between the two scenarios can be attributed to these constructions on the floodplain. Figure 3.4 shows the location of the study area.

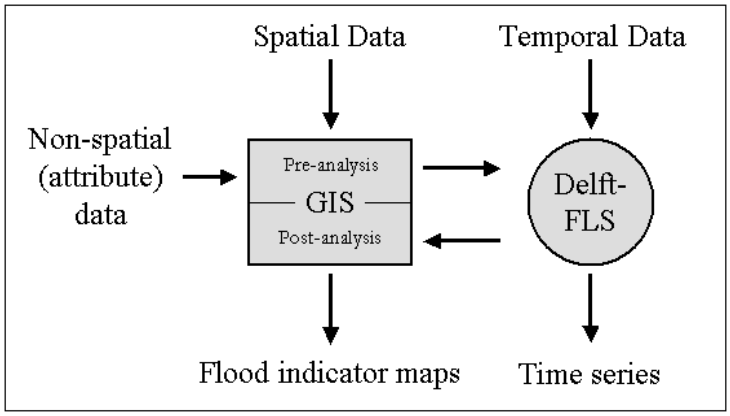

Figure 3.3. The use of a GIS in parallel with the flood model to process input and output data.

The model needs the following input data (see e.g. Stelling et al. 1998 and Stelling, 2000):

Spatial data

- Elevation;
- Surface roughness.

Temporal data

- Initial water levels;
- Upstream and downstream boundary conditions (water levels, fluxes, ..);
- User-defined dike breach evolution and final breach geometry (if applicable).

A scenario is defined in the so-called Master Definition File (mdf), which is a text-file that contains all instructions required by the program to run the simulation – see Stelling (2000). It also contains options for the output generation.

Spatial data

The elevation map has to contain all surface elements that can affect the flow of water, even features that are not included in regular digital terrain models (DTM) like dikes, embanked infrastructure, large buildings or riverbed morphology.

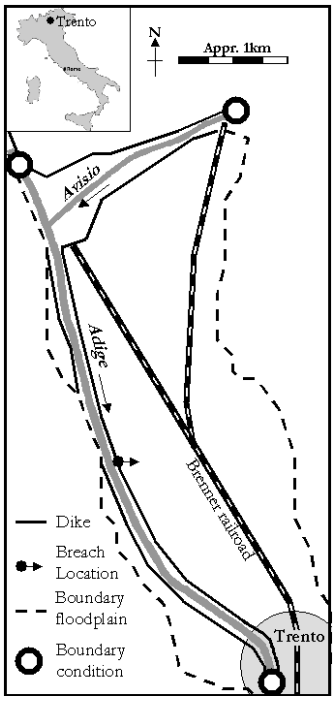

Figure 3.4. Location of the study area.

Many of these features have to be extracted from topographical maps, building footprints maps, field surveys, river cross-sections or bathymetry data and other sources. All these data layers need to be integrated to create the final Digital Surface Map (DSM) that contains all flow influencing objects, like terrain elevation, height and location of dikes and embankments and location of tunnels and bridges. Delft-FLS reads this DSM in standard ArcInfo asci (.asc) format with regularly spaced cells (grid) that contain the elevation values. The computation time largely depends on the number of cells in the grid, so for a given area it is advisable to generate the DSM at several resolutions to find a balance between resolution, number of grid cells and computation time. Another aspect that has to be considered in the choice of the grid-size is the fact that the model only computes flow in the direction of the 4-connected cells and not to the diagonally (8-) connected cells. For the representation of street networks and channel systems this may impose restrictions on the grid-size, especially in urban areas. In the procedure to generate the DSM, the connectivity of the street network should be checked. A different problem arises when the DSM is derived from a Laser Altimetric Survey (or LIDAR). This kind of DSM contains all surface features at very high resolution

(often in the range of 1m) with a very high accuracy (in the range of centimetres). So in principle it is a very suitable basis for flood modelling. However, its high resolution, and consequently large number of grid-cells for larger areas, makes it impossible to feed it directly into the flood model, because the calculation time would become enormous. In this case a procedure has to be developed in the GIS to decrease the resolution without loosing the exact height information of critical flow-influencing objects (like dikes, embankments, etcetera). An example of such a procedure is given in Chapter 4.
Similarly, the surface roughness map has to be generated at the same resolution as the DSM to ensure that for each cell both elevation information and roughness values are available. Often the surface roughness map is derived from a land-cover or land use map. If these are not available, interpretation and classification of remotely sensed imagery (airborne or satellite based) can assist. In literature tabulated data exist that give values of roughness coefficients (usually Manning's coefficient) as a function of the land-cover, which can then be linked to the land-cover maps as attribute data, to generate a spatial representation of the roughness coefficients (see e.g. Chow, 1957; Barnes, 1967; Arcement and Schneider 1990).

The Provincial authorities of Trento (*Servicio Urbanistica*) provided the DTM, as well as the footprints of current buildings and the location of infrastructures. The elevation data was provided in grid-format with a grid size of 10 metres. During a field survey this data was complemented with information regarding the height of embankments and dikes. The bathymetry of the Adige River and its tributary the Avisio River was derived from cross-sections provided by the Authority of the Adige Basin. All data were integrated into two final Digital Surface Models, one with the 1966 topography and one representing the 2000 situation - see Figure 3.5. Comparison between the 1966 and 2000 topography reveals that large parts of the alluvial plain of the Adige and the alluvial fan of the Avisio have undergone significant transformations. Many new buildings and some major infrastructure were constructed in that time period, like a large industrial area North of Trento, a transit zone "*Interporto*" near the confluence of the Avisio and Adige, the Brenner highway and the Trento by-pass road.
The land-cover map made by Geneletti (2001) was used to obtain the spatial distribution of surface roughness coefficients, using the values of Manning's coefficient for the various land-cover types. These were obtained from Chow (1959) and Selby (1989) – see also section 6.2.

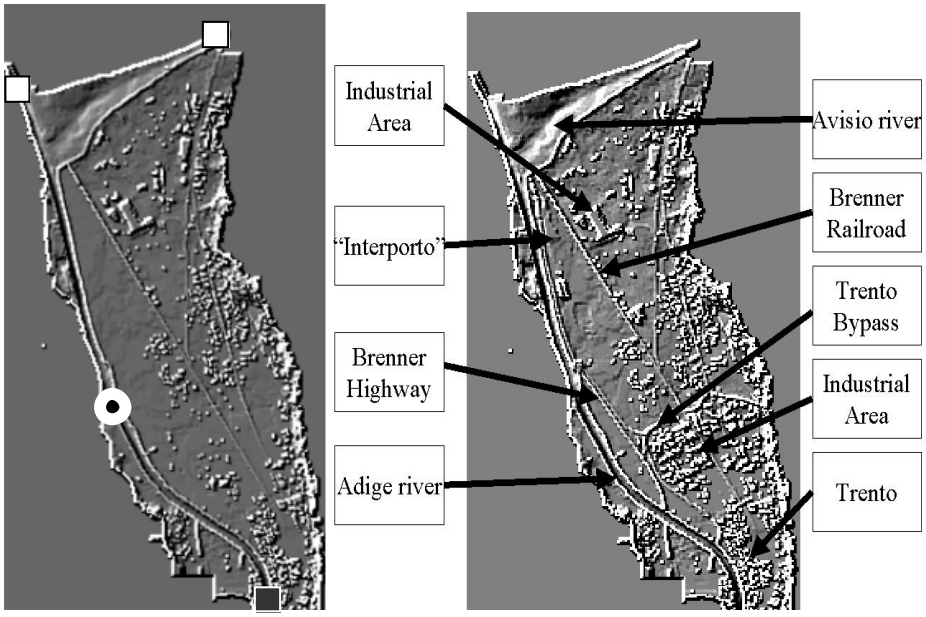

Figure 3.5. *(left) The surface topography in 1966. The dot indicates the location of the dike breach. (right), The white squares indicate the two upstream (discharge) boundaries (define the flow into the area) and the black square indicates the downstream (Q-h) boundary. (right) The detailed Digital Terrain Model representing the 2000 topography with some important topographical features. "Interporto" indicates a newly developed transit zone for cargo transfer from road to rail and v.v.*

Temporal data

There are to sets of temporal data required for a model run: 1) The initial conditions and 2) the boundary conditions.

Ad 1) Initial conditions.

The initial conditions describe the state of the system (water levels and fluxes) at the start of the computation. They can be defined in two different ways: 1) imposed by the modeller, and 2) calculated by Delft-FLS during a pre-modelling run, which creates a so-called restart file. In the second option the pre-simulation run starts at dry conditions and slowly water is added to reach a hydraulically stable starting point for the flood simulations. In this study for all scenarios restart files were constructed.

Ad 2) The boundary conditions

The boundary conditions describe the exchange of water mass between the study area and the rest of the universe during the model run. At these points (see Figures 3.4 and 3.5) is defined how much water enters the area and how much is leaving downstream. The upstream boundaries usually consist of time-series with water levels (m) or with discharges (m^3/s). The downstream boundaries are usually water levels (in the case of a lake or the sea) or a rating curve. This last option is the site-specific relationship between water levels and discharge (also known as Q-h relationship). In the case where the river continues beyond the downstream the rating curve is the preferred lower boundary condition, although it increases the computation time. The boundary conditions are in the form time-series tables of discharge (or water levels) or in a table with the relationship between water level (h) and the discharge (Q).

In the case of a dike breach, the modeller must define the location and development of the breach. Each raster cell that is part of the breach must be identified and linked to a file that contains the information on how much that raster cell is "lowered" as a function of time. For large breaches that cover multiple cells, the breach evolution can thus be reconstructed in detail.

The Basin Authority of the Adige River provided the discharge information of the Adige River (station San Michele) and the Avisio River (station Lavis) that are shown in Figure 3.6 as well as the rating curve of the Adige River at Trento (Figure 3.7). According to information from the Basin Authority (Mr. Bordato, oral communication) the estimated design discharge of the Adige protection works in the stretch between Avisio and Trento is approximately 1200 m^3/s. According to the graphs in Figure 3.6 this maximum discharge was reached at t = 10 hours, just before the peak discharges of both the Adige and Avisio. In the simulations, the breaching of the dike coincided with the moment of peak discharge (t = 10 hours) and based on information from past dike breaches (Adige Basin Authority; Mr. Bordato - oral communication) the maximum width of the breach was set to 50 meters wide (5 grid cells). In absence of reliable breach geometry information the maximum depth of the breach as assumed to be 4 meters (below the original height) which it reached at t = 12 hours.

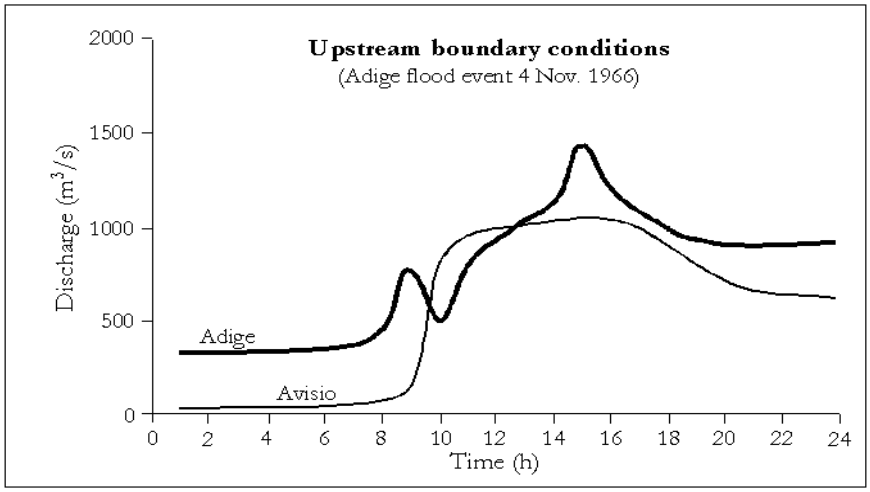

Figure 3.6. Discharges of the Adige and the Avisio during the 1966 flood.

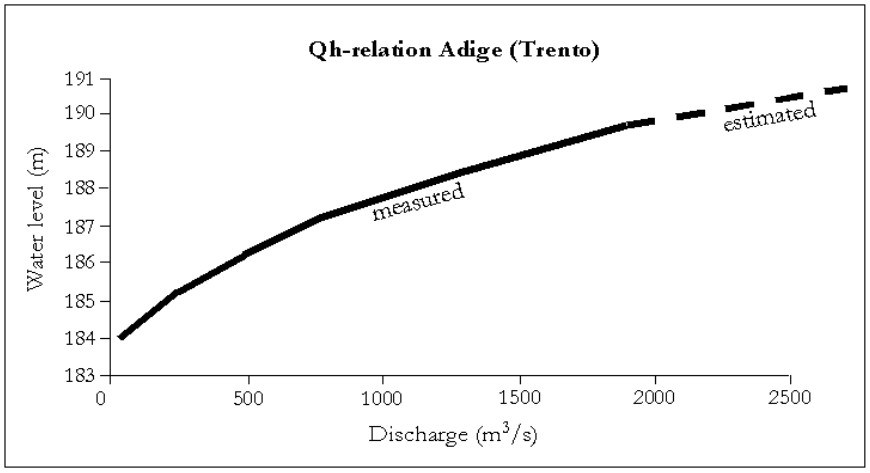

Figure 3.7. Q-h relationship – or rating curve – of the Adige at Trento.

3.5 Output data and generation of parameter maps

Delft-FLS generates three types of output: 1) dynamic output, 2) temporal output and 3) spatial-temporal output.

Ad 1) The dynamic output is in the form of an incremental flood animation file that can be visualised with a special software, Quickin, also developed by WL|Delft Hydraulic. This software is provided together with Delft-FLS and show the flood propagation as a video-animation.

Ad 2) The temporal output consists of tables with time-series of water depth at predefined locations and of discharge at predefined cross-sections.

Ad 3) At predefined time intervals maps are generated that show the spatial distribution of water depth and flow velocity. At the end of the simulation additional maps are created that contain the maximum water depth and flow velocity that occurred at each cell during the simulation.

Parameter maps
Although the dynamic and temporal outputs are very instructive and useful for various purposes (see e.g. Chapter 4), the most import information for hazard and risk assessment is contained within the map-series with water depth and flow velocity. These stacks of maps are saved in asci-format and must therefore be imported into a GIS for further analysis and visualization (see Figure 3.3). For a lengthy flood simulation these stacks can contain over a hundred files. To analyse this data an aggregation procedure has been developed to create 6 parameter maps that describe the different aspects of the flood event. Apart from the maps with the maximum water depth and flow velocity these parameter maps are (see Figure 3.8):

- Maximum impulse
- Maximum rising of the water level
- Flood propagation characteristics (also Warning time)
- Duration

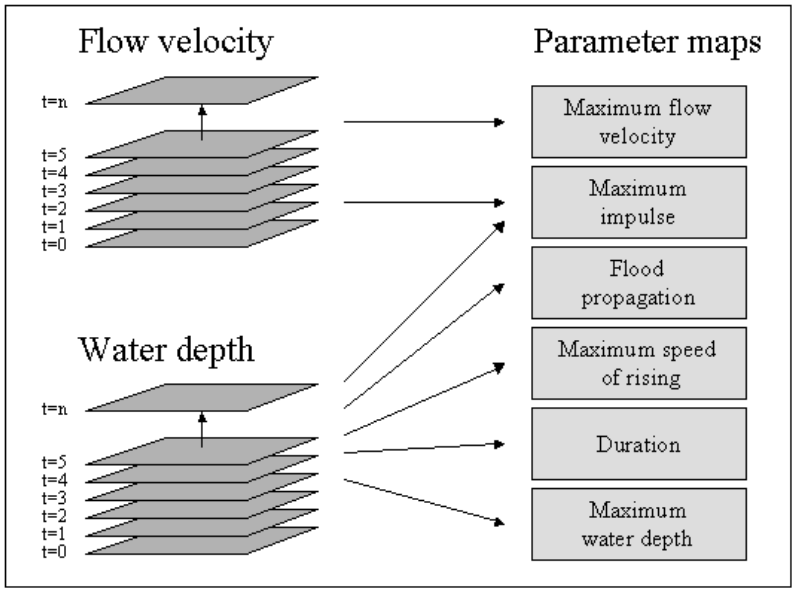

Figure 3.8. Transformation of the model output maps into flood hazard parameter maps. The colour coding shows how these parameter maps were used for the risk / damage assessment.

1 **Maximum water depth** (unit: m);

This map shows the maximum depth that occurred during the inundation. The rationale behind this parameter map is that areas with deep water are more dangerous to people and potentially more damaging to objects like houses and cars. It identifies areas where the second floor of houses, or even the third or fourth floor, is not a safe refuge. The maximum water depth map also serves as a possible means for model calibration. Maximum water depth is one of the few flood parameters that can easily be retrieved after a flood event because of wetting marks in and on houses.

2 **Maximum flow velocity** (unit: m/s);

This map shows the maximum flow velocity that occurred during the inundation. The rationale behind this parameter is that velocity is a component of the floodwater that can sweep people off their feet and make cars float away. This map shows where preferential flow paths may develop that could be dangerous for children, adults and cars.

3 **Maximum impulse** (unit: m^2/s);
This map shows the maximum impulse that occurred during the inundation. The impulse is calculated at each time step by multiplying water depth and flow velocity. For each pixel this value represents the amount of movement of the water mass (per pixel the mass only depends on the water depth, since the surface area of the pixel and volume weight of water are constant). The rationale behind this parameter is that flow velocity alone does not suffice to estimate the amount of potential damage or danger to humans and cars to be swept away. Shallow water with a high flow velocity does not have a lot of kinetic energy or momentum and neither has deep, but practically still-standing water. Deep, fast flowing water however is potentially dangerous for people and vehicles and is potentially damaging to objects like houses and crops.

4 **Maximum rising of the water level** (unit: m/h);
This map shows the maximum speed at which the water level rose at some point during the inundation. It is calculated by taking the difference between two successive water depth maps, divided by the time interval between the two maps. The result is an increase in water depth per hour. The rationale behind this parameter map is that a quick rising of the water level is potentially dangerous for people who may not have sufficient time to seek higher ground or elevated structures.

5 **Flood propagation characteristics** (unit: h);
This map shows how the flood propagates through the area. After each time interval the flooded area is identified and compared with the situation at the previous time interval. It records the time at which a cell is inundated for the first time. The rationale behind this parameter map is that it shows how much time it takes for the first floodwater to reach a certain location and thus how much warning time people have to prepare themselves. Areas that are flooded quickly are potentially more dangerous than areas further away.

6 **Duration** (unit: h).
This map estimates the time the floodwater remains at a certain location. It is based on several assumptions regarding the drainage of the floodwater from the flooded area. For instance in the studies presented in this book it is assumed that there is free drainage at the lowest point of the inundated area through a "canal" of

a certain width (1 or more pixels wide). It also requires a sufficiently long simulation run that includes the descending limb of the flood wave. The rate of water level change is calculated as dh/dt, where dh is the difference between the maximum water depth and the water depth at the end of the simulation and dt is the difference between the time at the end of the simulation and the time the maximum water depth is reached. The duration is estimated by extrapolating this rate of change until the moment of a water depth of zero is reached - see Figure 3.9.

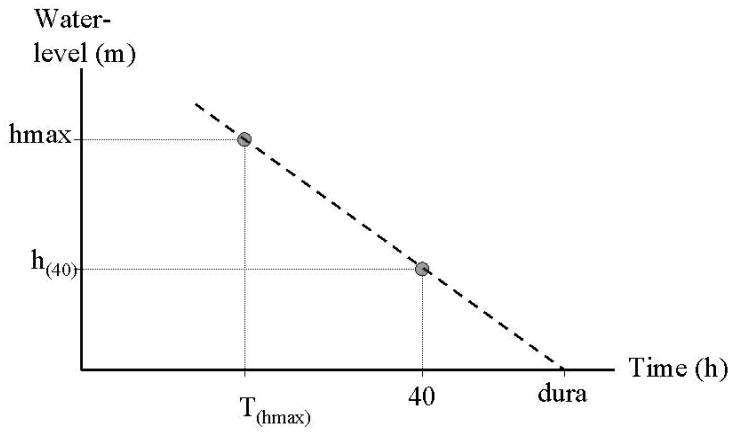

Figure 3.9. Estimation of the parameter "duration".

The rationale behind this parameter is that it gives a first, rough impression of how long the floodwater will stay in the area. This is the minimum time period that people have to be relocated, that businesses and industries are closed and that transportation in and through the area might be impossible or hindered. It is a strong parameter to assess the economic and social impact of the flood on the people living and working in the area. It is also an important parameter to estimate agricultural damage because many crops, like fruit bearing trees and vineyards can withstand inundation of their stems for a short time (usually some days), but if the period becomes too long the roots will starve from oxygen depletion and the trees will die.

Note: because of the longer simulation period required to compute the recession of the water level in the area, the duration was not calculated for this example.

3.6 Analysis of the results

For the example study of Trento, the first five parameter maps have been computed for the 1966 as well as for the 2000 topography. Figure 3.10a-c shows the results for both scenarios. The third map for each parameter shows the difference between the two scenarios (the 2000 results are subtracted from the 1966 results). Because all other parameters remained unchanged, the differences can be attributed to the topographical changes on the alluvial plain. The results show that these developments have a significant effect on all parameter maps. In some places maximum water depth was reduced, in other places it increased. The same holds for flow velocity, impulse, speed of rising of the water level and propagation of the inundation. To make things more complicated, the changes do not show the same spatial pattern. Where one parameter gives an improvement (less hazard) the other parameter shows a worsening of the situation (more hazard). Looking carefully at Figure 3.10 the following observations can be made:

- The Brenner Highway (see Figure 3.5) creates a sub-compartment directly behind the breach which results in an increase of water depth, impulse and rising of the water level;
- Also elsewhere, sub-compartments were created by embanked infra-structures which has significant consequences, especially for the speed with which the water level rises;
- Tunnels, bridges and other "connections" between compartments, create locally higher flow velocities and impulse;
- The obstruction to flow by elevated infrastructure and by buildings on the plain has decreased the flow over the plain downstream (South), thereby increasing the water depth and decreasing the warning time (flood propagation time) in the Northern part.

It is concluded that man-made objects like roads and railroads compartmentalise the floodplain and that the propagation of the flood follows these compartments as can be seen in Figure 3.10 that shows the flood propagation map. Another general conclusion is that tunnels, bridges, buildings and other man-made topographical elements funnel the floodwater through narrow passages, resulting in high flow-velocities and high impulse at these locations. The issue of how to continue with this multi-parameter flood hazard and risk assessment is discussed further in Chapters 6 and 8.

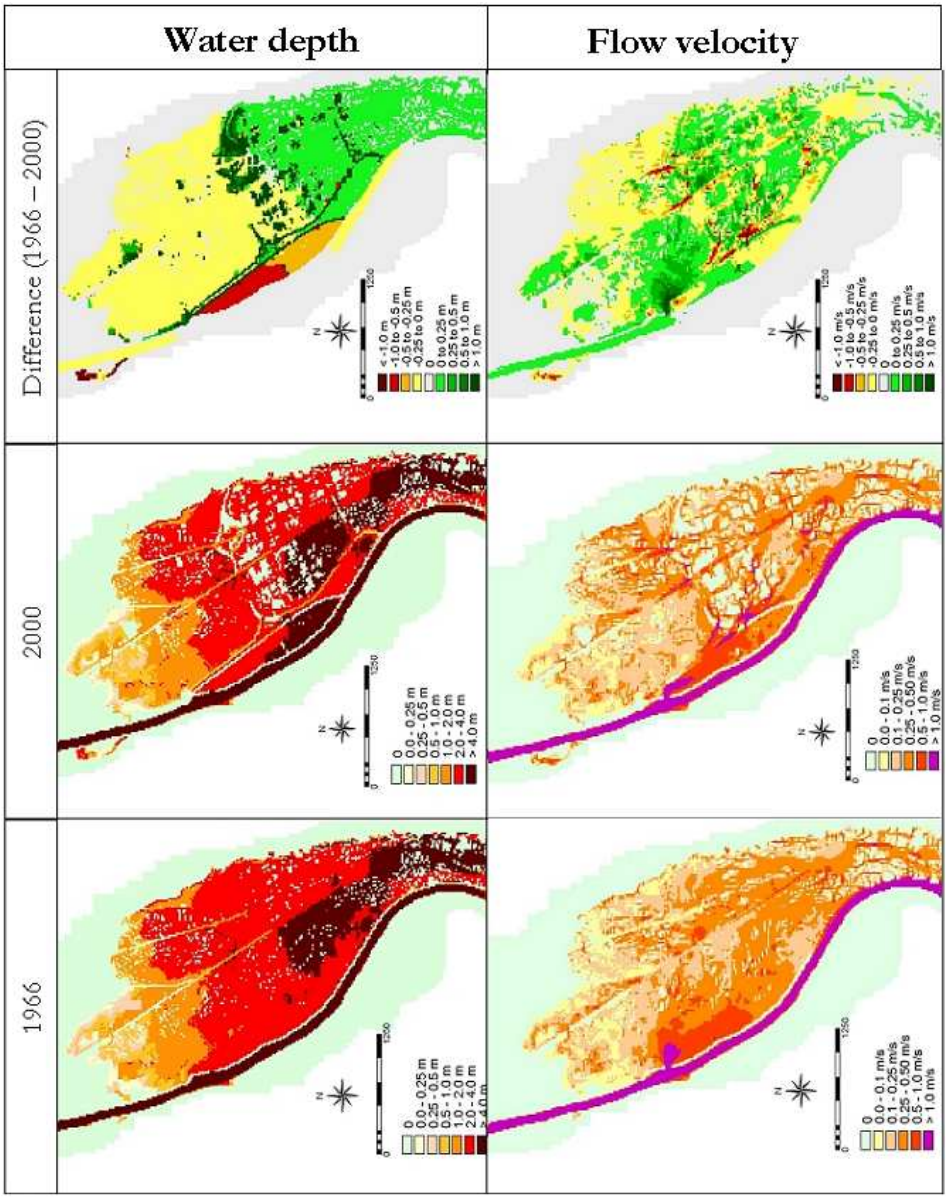

Figure 3.10a. Parameter maps water depth and flow velocity.

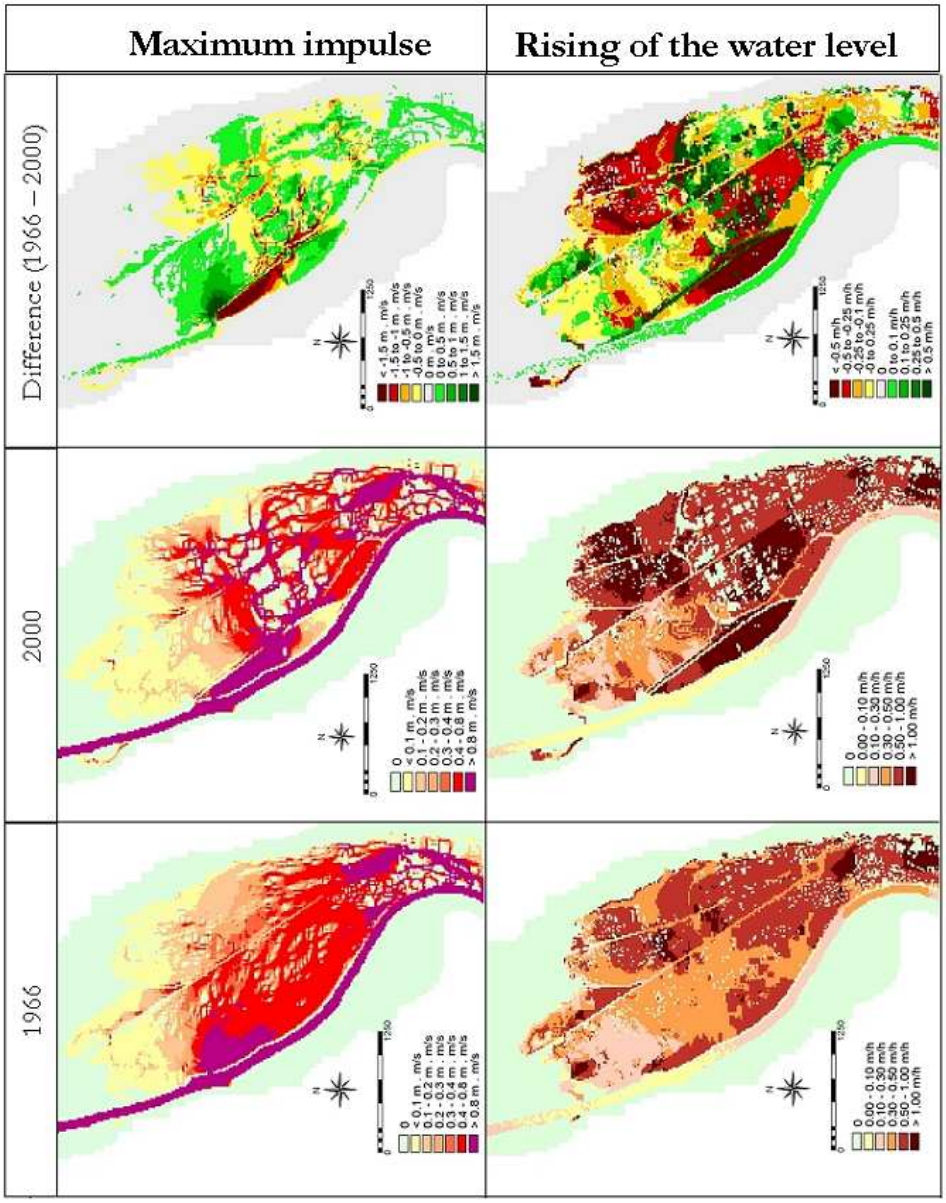

Figure 3.10b. Parameter maps impulse and rising of the water level.

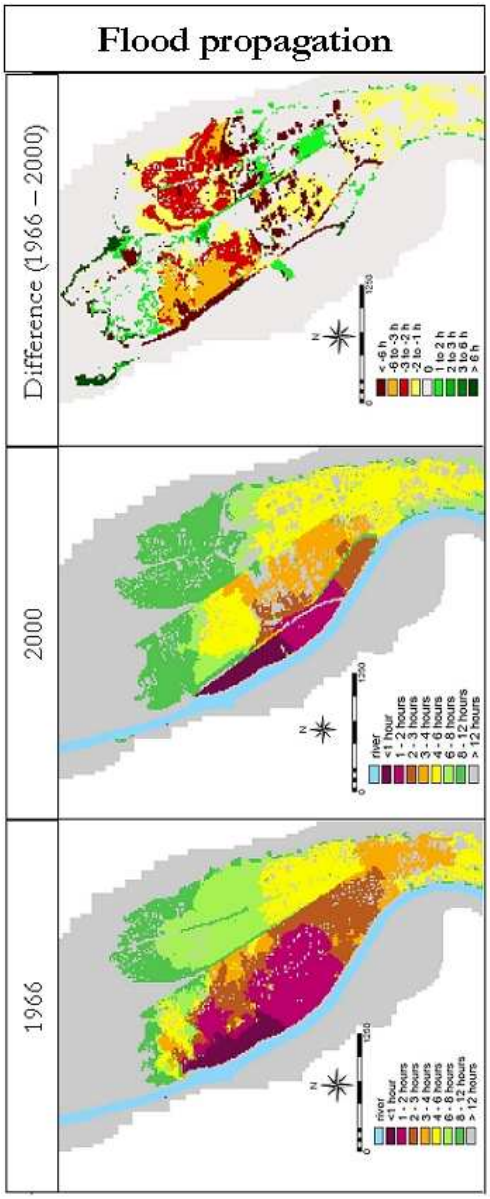

Figure 3.10c. Parameter map flood propagation

3.7 Model testing

There are three ways of testing a flood inundation model (see e.g. Hesselink et al. 2003):

- to test the numerical scheme of the model by comparison with analytical solutions and theoretical analyses of consistency, stability and convergence;
- by comparing the model simulation results with tightly controlled laboratory inundation experiments, (see e.g. Stelling and Verwey, 2005);
- by comparing the model simulation results with real-world flood events (Hesselink et al, 2003).

Until now, very few studies have been made to evaluate the performance of inundation models with real-world flood events. This is mainly due to model complexity and lack of real-world measurements. The information that is available after a flood is usually in the form a water level marks – or wetting marks, that give the local flood depth. Although these are important for model testing, they are not sufficient to test a 2D flood propagation model properly. To do this additional measurements are needed regarding the 'dynamic' characteristics of the flood like arrival time of the flood water, flow velocity and speed of rising of the water level. These are usually not available after a flood event. Hesselink at al. (2003) give an example of a real-world test with Delft-FLS which was used to simulate the 1805 inundation of a Dutch river polder and to compare the results with historic water level data. Among their conclusions was that such studies can be used to evaluate the model performance for real inundations, even for events with long return periods. In Chapter 4 another real-world event is reconstructed to test Delft-FLS.

3.8 Conclusion

This chapter presents the theoretical and practical basis for flood modelling in (nearly) flat terrain with complex topography. It is argued that in "polder" situation no linear relationship exists between water levels and probability of occurrence (return period) of a flood. For these areas traditional hazard maps are not very informative if the hazard is defined as the probability that an area is flooded. This

will result in large uniform areas with a probability of flooding (hazard) that is equal to probability of bank-full discharge of the river or the design characteristics of the protection works. In order to differentiate the hazards within the polder additional information is needed regarding the flood propagation, maximum water depths, flow velocities etc. To obtain this information 2D flood models can be applied to simulate the flow of water over (nearly) flat terrain and complex topography. The example of the Adige river near Trento demonstrates the application of Delft-FLS and shows what data is required to run the model and how the model results can be transformed into a set of flood parameter maps: 1) the maximum inundation depth, 2) the maximum flow velocity, 3) maximum impulse, 4) maximum speed of rising of the water level, 5) estimated duration of the inundation and 6) the propagation of the flood water (or warning time).
In the Trento example it is made clear that Delft-FLS can be used to assess the effects of terrain modifications on the characteristics of the flow. Differences between the 1966 and 2000 simulation can be attributed to the construction of new infrastructures, industrial sites and other major changes in topography. Unfortunately no historic data was available to test the model results regarding its prediction performance. This issue will be addressed in the next chapter.